

# Towards Modelling a Diphasic Flow Using the CFD Technique to Achieve a Digital Twin of a Phosphate Slurry Piping Process

Marwane Elkarii<sup>a</sup>, Chakib Bouallou<sup>b,\*</sup>, Ahmed Ratnani<sup>a</sup>

<sup>a</sup>Laboratory of CSEHS, University Mohammed VI Polytechnic, Ben Guerir, Morocco.

<sup>b</sup>MINES ParisTech, CES - Centre Efficacité énergétique des Systèmes, 60, Bd Saint-Michel 75006 Paris  
 chakib.bouallou@mines-paristech.fr

This work concerns the transport of phosphate ores in the context of an industry 4.0. The process begins with the extraction of the ore, that is transported as pulp (Water + Phosphate) in a pipeline from the mine to the industrial units for its valorization to fertilizers. The phosphate pulp is transported in batches, separated by batches of water to control the quality and the flow of the pulp. The present work aims at developing and assessing a numerical model for solid-liquid mixtures using OpenFoam software, in order to investigate and control the dynamic behaviour of phosphate slurry flows under isothermal conditions. A Eulerian multiphase approach was used, where both liquid and solid phases are considered as continua. The Eulerian model is the most complex and computationally intensive among the multiphase models. It solves a set of momentum and continuity equations for each phase. Coupling is achieved through the pressure and interphase exchange coefficients. To describe particulate flow stresses, the kinetic theory of granular flow (KTGF) was employed. Model validation is demonstrated on a test case of pure sedimentation of suspended particles, for which the concentration profile data is reported in the literature.

## 1. Introduction

Particle transport through pipelines is an important operation in many industries, including the food, pharmaceutical, chemical, petroleum, mining, construction and energy production industries, since on the one hand, it can be more efficient with regard to long distances. On the other hand, pipelines are more environmentally friendly than rail with 77 % fewer greenhouse gas emissions than rails (Nimana et al., 2016). But in many such applications, the carrier fluid may be highly viscous and have Newtonian or non-Newtonian rheology and generally turbulent flow (Lahiri et al., 2010). Researchers around the world have been seriously concerned with predicting velocity, concentration profiles and pressure drop in slurry pipelines over the years (Chen et al., 2009). Most of the equations available in the literature for predicting solid concentration profiles in the slurry pipeline are empirical in nature, and they are usually developed based on limited data, besides their limited applicability (Sultan et al., 2019). Computational Fluid Dynamics (CFD) has emerged as a useful and powerful tool to model and predict unknown or particular slurry flow scenarios (Xia et al., 2002). The criterion for success is to what extent the results of the numerical simulation agree with the experience in cases where careful laboratory experiments can be established.

Modelling liquid-solid slurry flows in pipelines has been successfully made for laterite and sand slurry by Bossio et al. (2009), sand and water slurry by Kaushal et al. (2012), ice slurry by Wang et al. (2013), silicone oil and Mono-dispersed spherical polystyrene beads mixture by Chauchat et al. (2017). In this study, the three-dimensional Reynolds Eulerian model is used to model the flow of a solid-liquid mixture in a fixed bed and sliding bed flows. The solid phase is modelled in this Eulerian framework as an interpenetrating fluid but with a viscosity that is determined by the kinetic theory of granular flows as in the previously cited works. In the past, numerical simulations have been performed for slurry flows in horizontal pipes with relative success in predicting flow properties such as particle concentration, velocity profiles for each phase and pressure drop. However, these predictions were made with moderate volumetric concentrations of solids, up to 45 % for Ekambara et al. (2009),

up to 50 % for Kaushal et al. (2012), and up to 25 % for Wang et al. (2013). Kaushal et al. (2013) confirmed that most of the previous studies on slurry pipeline systems are based on moderate volumetric concentrations of solids (25 % - 40 % by volume). This work aims to develop a model that deals with high volume concentrations, since they usually show more complicated behaviour, which is the case for the transport of the phosphate slurry, that has a solid concentration that goes up to 65 %. In this case, the validation of the model and its capability to reproduce and predict high volume concentration profiles was carried out with a solid volume concentration of 60 %. Concentration profiles of particles are compared with experimental data from Chauchat et al. (2017).

## 2. Mathematical Model

The resolution of a two-phase problem consists in solving equations of fluid dynamics, and coupling between different phases is carried out by relations taking into account the exchanges of matter, momentum and energy. To process this resolution, there are two approaches (Sokolichin et al., 1997). The first one is the Euler-Lagrange approach which consists in following discrete particle trajectories present in a continuous carrier phase, by solving the equations of point mechanics for the particles that are subjected to the forces exerted by the carrier phase. The second one is Euler-Euler, where different phases are treated as continuous which can interpenetrate, by introducing the notion of volume fraction of phases. This approach does not seek to determine the properties of each particle present in the flow, but to calculate local properties of the two-phase flow. As the phosphate slurry flow has a high solid concentration, the second approach will be adopted, yet three models are possible. Table 1 shows a comparison of the latter models.

Table 1: Comparison between Euler-Euler models

VOF	Mixture Model	Eulerian Model
Modelling non-miscible fluids.	Model used if there is a wide distribution of dispersed phases.	Interphase laws available.
A single set of motion equations.	Interphase laws not available.	More precise.
Examples: free surface flow (Jing et al., 2016), large bubbles in a liquid (Al-Yaari et al., 2011), stratified flow (Akhtar et al., 2007).	Examples: particle-laden flow* with low load (Dufek et al., 2007), bubble flow, sludge flow (Chen et al., 2004).	Examples: sludge flow (Ofei et al., 2016), sedimentation (Gopaliya et al., 2016), fluidized beds (Ofei et al., 2014).

\*Particle-laden flow = Particle charge flows refer to a two-phase flow in which one of the phases is continuously connected and the other phase consists of small immiscible particles and typically diluted.

Two-phase Eulerian model adopted in present research assumes that the slurry flow consists of solid phase S and water phase W. These phases are assumed to be separated yet forming interpenetrating continua such that  $\alpha_S + \alpha_W = 1$ . where  $\alpha_S$  and  $\alpha_W$  are the volumetric concentrations of solid and fluid phases. Continuity and momentum equations are individually satisfied by each phase. The coupling of these equations is achieved using pressure and interfacial exchange coefficients - (Vittorio Messa et al., 2014) for solid-liquid slurries, and (Chauchat et al., 2017) for sediment transport. Solid-phase viscosity is determined using KTGF, which is based on the kinetic theory of gases in a generalized way, in order to take into account collisions of inelastic particles, to define a granular temperature in the solid phase which directly affects the phase stress tensor (Gonzalez et al., 2014).

Assuming an isothermal, homogeneous, incompressible flow, and there is no phase change or chemical reactions between the two phases slurry/water, the source term is then expressed by Eq(1):

$$\sum_1^N (\dot{m}_{sw} - \dot{m}_{ws}) = 0 \quad (1)$$

The lift forces will be neglected considering that the slurry phase is composed of very small particles, and the virtual mass forces will also be neglected considering that there is not much difference in density between the two phases. The Slurry transport model was detailed in (Lahiri et al., 2010). The continuity equations for both phases are given by Eq(2) and Eq(3):

$$\frac{\partial(\alpha_W \rho_W)}{\partial(t)} + \nabla \cdot (\alpha_W \rho_W v_W) = 0 \quad (2)$$

$$\frac{\partial(\alpha_S \rho_S)}{\partial(t)} + \nabla \cdot (\alpha_S \rho_S \mathbf{v}_S) = 0 \quad (3)$$

The momentum equations for both phases are given by Eq(4) and Eq(6), while the stress tensors for both phases are expressed by Eq(5) and Eq(7):

$$\frac{\partial(\alpha_W \rho_W \overline{\mathbf{v}_W})}{\partial(t)} + \nabla \cdot (\alpha_W \rho_W \overline{\mathbf{v}_W} \overline{\mathbf{v}_W}) = -\alpha_W \nabla P + \nabla \cdot \boldsymbol{\tau}_W + \alpha_W \rho_W \overline{\mathbf{g}} + (K_{SW}(\overline{\mathbf{v}_S} - \overline{\mathbf{v}_W})) \quad (X,t) \in \Omega \times (0,T) \quad (4)$$

$$\boldsymbol{\tau}_W = \alpha_W \mu_W (\nabla \mathbf{v}_W + (\nabla \mathbf{v}_W)^T) - \alpha_W (\lambda_W - \frac{2}{3} \mu_W) (\nabla \cdot \mathbf{v}_W) \mathbf{I} \quad (5)$$

$$\frac{\partial(\alpha_S \rho_S \overline{\mathbf{v}_S})}{\partial(t)} + \nabla \cdot (\alpha_S \rho_S \overline{\mathbf{v}_S} \overline{\mathbf{v}_S}) = -\alpha_S \nabla P + \nabla \cdot \boldsymbol{\tau}_S + \alpha_S \rho_S \overline{\mathbf{g}} + (K_{WS}(\overline{\mathbf{v}_W} - \overline{\mathbf{v}_S})) \quad (X,t) \in \Omega \times (0,T) \quad (6)$$

$$\boldsymbol{\tau}_S = \alpha_S \mu_S (\nabla \mathbf{v}_S + (\nabla \mathbf{v}_S)^T) - \alpha_S (\lambda_S - \frac{2}{3} \mu_S) (\nabla \cdot \mathbf{v}_S) \mathbf{I} \quad (7)$$

$\Omega$  is the computational bounded domain which is a pipe included in  $\mathbb{R}^3$  with boundary  $\partial\Omega = \text{Inlet} \cup \text{Lateral surface} \cup \text{Outlet}$ .  $[0, T]$  is a time interval with  $T$  is the time of the simulation.

$\alpha_W$ : Volume fraction of water and  $\alpha_S$ : Volume fraction of slurry, With  $\alpha_W + \alpha_S = 1$

$\rho_W$  and  $\rho_S$  are the densities of water and slurry

$P$ : Pressure shared by all phases

$\boldsymbol{\tau}_W$ : Stress-strain tensor of the water phase

$\boldsymbol{\tau}_S$ : Stress-strain tensor of the slurry phase

$K_{SW}/K_{WS}$ : The exchange coefficient of momentum between water and slurry

$N$ : Total number of phases

$\overline{\mathbf{v}_W}$ : Water velocity and  $\overline{\mathbf{v}_S}$ : Slurry velocity

The Slurry-Water exchange coefficient  $K_{SW}$  has the general form given by Eq(8), - see (Visuri et al., 2012) for fluidised beds and (Lahiri et al., 2010) for slurry modelling:

$$K_{SW} = \frac{\alpha_S \rho_S f}{\tau_S} \quad (8)$$

Where  $f$  is the drag function as expressed in Eq(9), it includes a drag coefficient (CD) based on the relative Reynolds number (Re) and is calculated in our case according to Schiller and Naumann's model as shown in Eq(10). The Schiller and Naumann model is the default method, and it is acceptable for general use for all fluid-solid phase pairs:

$$f = \frac{CD \text{ Re}}{24} \quad (9)$$

Where,

$$CD = \begin{cases} 24(1+0.15\text{Re}^{0.687}) & \text{Re} \leq 1000 \\ 0.44 & \text{Re} > 1000 \end{cases} \quad (10)$$

And Re is the Reynolds number defined by Eq(11):

$$\text{Re} = \frac{\rho_W |\overline{\mathbf{v}_S} - \overline{\mathbf{v}_W}| d_S}{\mu_W} \quad (11)$$

$\tau_S$  is the relaxation time of particles calculated by Eq(12):

$$\tau_S = \frac{\rho_S d_S^2}{18\mu_W} \quad (12)$$

With  $d_S$  is the particular diameter of the slurry phase.

The solid-phase stress tensor in Eq(7) contains shear and bulk viscosities arising from particle momentum exchange due to collisions expressed in Eq(14), translations in Eq(15), and frictions given by Eq(16), these components are added to give the solid shear viscosity represented by Eq(13):

$$\mu_S = \mu_{S,col} + \mu_{S,kin} - \mu_{S,fr} \quad (13)$$

$$\mu_{S,col} = \frac{4}{5} \alpha_S \rho_S d_S g_{0,SS} (1 + e_{SS}) \left( \frac{\theta_S}{\pi} \right) \quad (14)$$

$$\mu_{S,kin} = \frac{10 \rho_S d_S \sqrt{\theta_S \pi}}{96 \alpha_S (1 + e_{SS}) g_{0,SS}} \left( 1 + \frac{4}{5} g_{0,SS} \alpha_S (1 + e_{SS}) \right)^2 \alpha_S \quad (15)$$

$$\mu_{S,fr} = \frac{Fr(\alpha_S - \alpha_{S,min})^n}{(\alpha_{S,max} - \alpha_S)^p} \sin(\phi) \quad (16)$$

After choosing the mathematical model necessary to simulate the diphasic flow, comes the part of the implementation under the OpenFOAM software. The twoPhaseEulerFoam solver is the one which represents well our model and since OpenFOAM is an open-source software the solver has been modified to become an isothermal flows solver. Then, in the constant file the different forces which act on the flow have been defined according to the assumptions made, where the interphase momentum exchange models have been defined. Then the components of the KTGF are implemented taking into consideration the restitution coefficients and the radial distribution function. The implementation of the model also requires special attention to the boundary conditions which need a good understanding of the physical phenomenon to define them.

### 3. Results and discussion

An attempt to simulate the behaviour of a sediment-water mixture during its transportation through a pipe has been made, using the twoPhaseEulerFoam solver available in the 6.0 release of the open-source CFD toolbox OpenFOAM. The geometry used consisted of a pipe of length  $L = 0.02$  m, a diameter  $D = 0.0001$  m. The flow is laminar with  $Re = 144$ ,  $\rho_S = 1,450$  kg/m<sup>3</sup> and  $\rho_W = 1,027$  kg/m<sup>3</sup>,  $V_{mixture} = 1$  m/s,  $d_S = 70$   $\mu$ m,  $\mu_W = 0.00891$  kg/m.s,  $\alpha_{0S} = 30\%$ ,  $P_0 = 10^5$  Pa. Figure 1a and 1b, shows the 2D and 3D meshed geometry. OpenFOAM's meshing utility blockMesh was used to generate structured orthogonal meshes about 200 cells along the pipe.

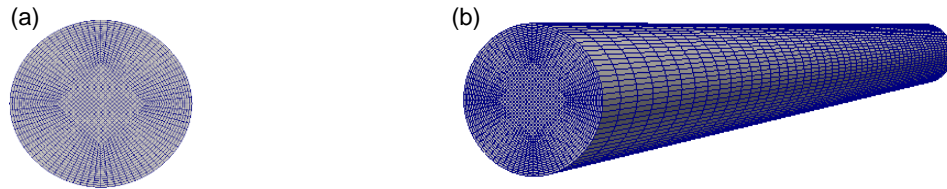


Figure 1: (a) Cross-section mesh (b) 3D pipe mesh

Figure 2a and 2b show the solid concentration for the cross-section of the pipe and along the pipe. These first results show an agreement with one of the types of two-phase flows found in the literature, which is a sliding bed flow. While, Figure 2c shows that the condition of the fractional volumes sum for the two phases is equal to 1, throughout the diameter of the pipe.

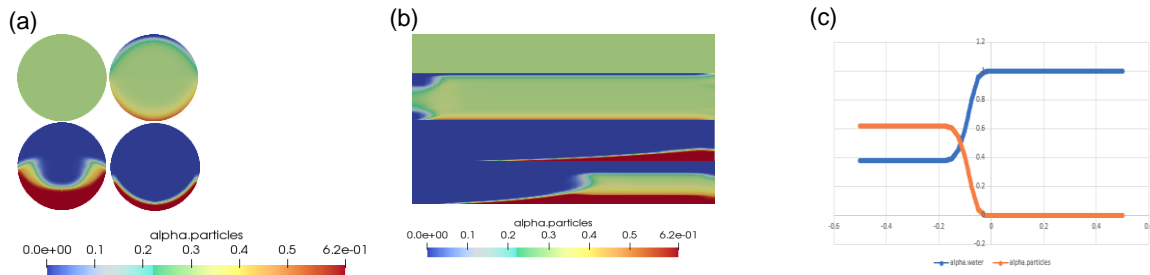


Figure 2: (a) Concentration for the cross-section (b): Concentration along the both pipe (c): Volume fraction of phases along the pipe diameter

The validation test case corresponds to a sedimentation of non-cohesive particles by Chauchat et al. (2017), based on experimental data from Pham Van Bang et al. (2008). The sediment phase is modelled as a continuum, and consecutive laws have to be prescribed for the sediment stresses. The intergranular stress model of the kinetic theory of granular flows is implemented. Details concerning the implementation, the initial and the boundary conditions, are found in Chauchat et al. (2017) and will not be further detailed. This validation test case on sedimentation of monodisperse spherical suspension allowed us to validate the numerical implementation of the pressure velocity coupling. Figure 3 shows the sediment concentration profiles evolution over time.

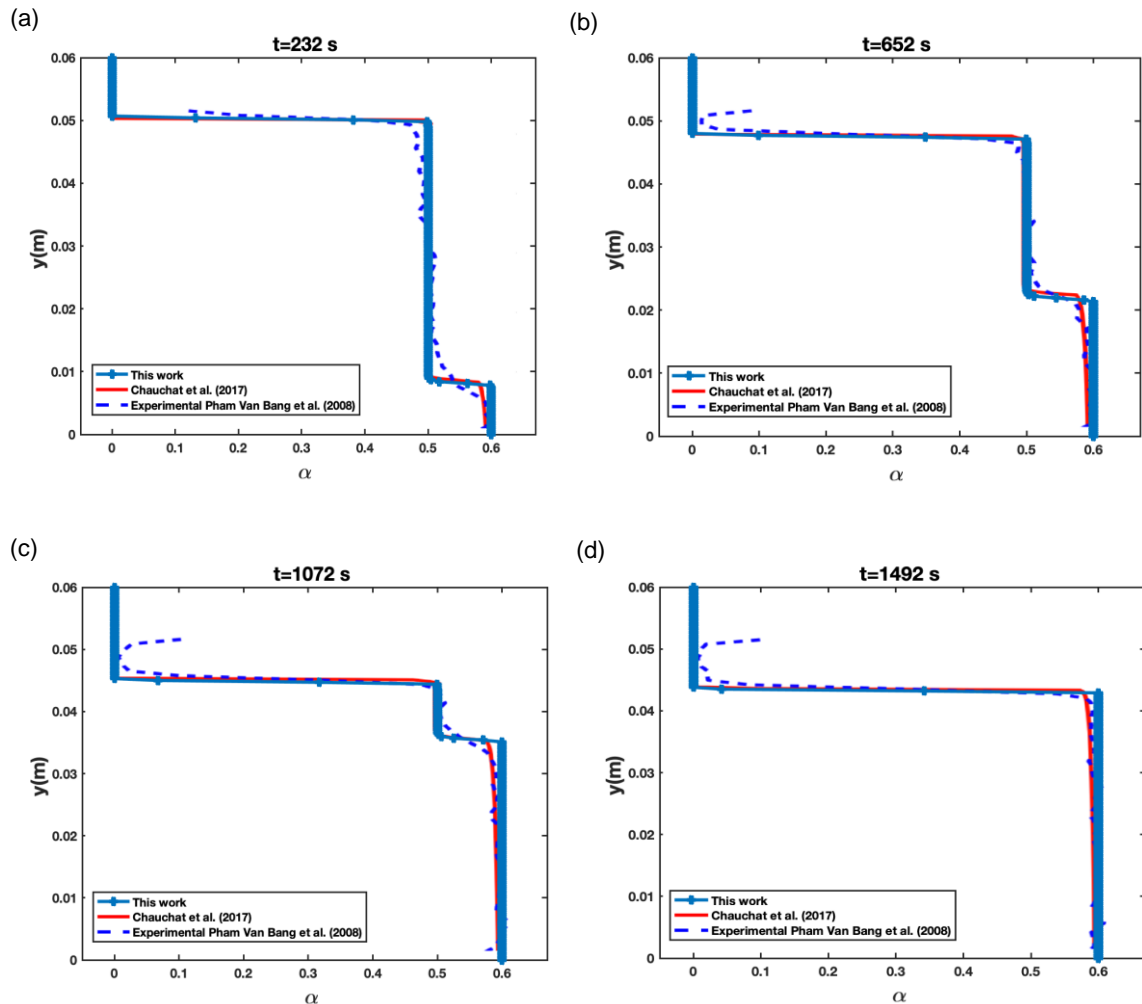


Figure 3: Sediment concentration profiles over time (a) At  $t = 232$  s, (b)  $t = 652$  s (c)  $t = 1,072$  s (d)  $t = 1,492$  s

#### 4. Conclusions

A Eulerian-Eulerian model using the kinetic theory of granular flow is developed to treat the dispersed solid phase as a fluid while taking into account the collisional, kinetic and frictional contributions into its viscosity. Preliminary results show that the multiphase OpenFOAM solver allowed us to integrate the solid phase and to sediment it in a two-phase flow after modification in the code. The first results on the simulation of solid sedimentation are in agreement with the regime simulated by CFD for a laminar flow which is a sliding bed flow. The validation test case of the sedimentation of monodisperse spherical suspension allowed us to validate the numerical implementation of the pressure velocity coupling, and to prove the capability of this solver to reproduce the sedimentation phenomena of particles in suspension, and its accuracy of prediction for high concentration profiles which will be useful in further study, to predict the concentration profile of the phosphate slurry flow.

## References

- Akhtar A., Pareek V., Tadó M., 2007, CFD simulations for continuous flow of bubbles through gas-liquid columns: application of vof method, *Chemical Product and Process Modeling*, 2, 1-19.
- Al-Yaari M.A., Abu-Sharkh B.F., 2011, CFD prediction of stratified oil-water flow in a horizontal pipe, *Asian Transactions on Engineering*, 1, 68-75.
- Bossio B.M., Blanco A.J., Hernández F.H., 2009, Eulerian-Eulerian modeling of non-Newtonian slurries flow in horizontal pipes, In: *Fluids Engineering Division Summer Meeting*, August 2–6, Vail, Colorado, USA, 1, 525-533, DOI: 10.1115/FEDSM2009-78019.
- Chauchat J., Cheng Z., Nagel T., Bonamy C., Hsu T.J., 2017, SedFoam-2.0: a 3-D two-phase flow numerical model for sediment transport, *Geoscientific Model Development*, 10, 4367-4392.
- Chen L., Duan Y., Pu W., Zhao C., 2009, CFD simulation of coal-water slurry flowing in horizontal pipelines, *Korean Journal of Chemical Engineering*, 26, 1144-1154.
- Chen P., Sanyal J., Dudukovic M.P., 2004, CFD modeling of bubble columns flows: implementation of population balance, *Chemical Engineering Science*, 59, 5201-5207.
- Dufek J., Bergantz G.W., 2007, Suspended load and bed-load transport of particle-laden gravity currents: the role of particle–bed interaction, *Theoretical and Computational Fluid Dynamics*, 21, 119-145.
- Ekambara K., Sanders R.S., Nandakumar K., Masliyah J.H., 2009, Hydrodynamic simulation of horizontal slurry pipeline flow using ANSYS-CFX, *Ind. Eng. Chem. Res.*, 48, 8159-8171.
- González J., Sabirgalieva N., Rojas-Solorzano L., Zarruk G., 2017, Numerical simulation of slurry flows in heterogeneous and saltation regimes in horizontal pipelines, *Chemical Engineering Transactions*, 57, 1279-1284.
- Gopaliya M.K., Kaushal D.R., 2016, Modeling of sand-water slurry flow through horizontal pipe using CFD, *Journal of Hydrology and Hydromechanics*, 64, 261-272.
- Jing L., Kwok C.Y., Leung Y. F., Sobral Y. D., 2016, Extended CFD–DEM for free-surface flow with multi-size granules, *International Journal for Numerical and Analytical Methods in Geomechanics*, 40, 62-79.
- Kaushal D.R., Thinglas T., Tomita Y., Kuchii Sh., Tsukamoto H., 2012, CFD modeling for pipeline flow of fine particles at high concentration, *International Journal of Multiphase Flow*, 43, 85-100.
- Kaushal D.R., Tomita Y., 2013, Prediction of concentration distribution in pipeline flow of highly concentrated slurry, *Particulate Science and Technology*, 31, 28-34.
- Lahiri K., Ghanta K.C., 2010, Slurry flow modelling by CFD, *Chemical Industry and Chemical Engineering Quarterly/CICEQ*, 16, 295-308.
- Moin P., Kim J., 1997, Tackling turbulence with supercomputers, *Scientific American*, 276, 62-68.
- Nimana B., Verma A., Di Lullo G., Rahman M. M., Canter C. E., Olateju B., Zhang H., Kumar A., 2016, Life Cycle Analysis of Bitumen Transportation to Refineries by Rail and Pipeline, *Environmental Science & Technology*, 51, 680-691.
- Ofei T.N., Irawan S., Pao W., 2014, CFD method for predicting annular pressure losses and cuttings concentration in eccentric horizontal wells, *Journal of Petroleum Engineering*, 2014, 1-16.
- Ofei T. N., Ismail A. Y., 2016, Eulerian-Eulerian Simulation of Particle-Liquid Slurry Flow in Horizontal Pipe, *Journal of Petroleum Engineering*, 2016, 1-10.
- Pham Van Bang D., Lefrançois E., Sergent P., Bertrand F., 2008, MRI experimentation and finite element modeling of sedimentation-consolidation of vessels (MRI experimentation and finite element modeling of sedimentation-consolidation of vessels), *La Houille Blanche*, 3, 39-44.
- Sokolichin A., Eigenberger G., Lapin A., Lübert A., 1997, Dynamic numerical simulation of gas-liquid two-phase flows Euler/Euler versus Euler/Lagrange, *Chemical Engineering Science*, 52, 611-626.
- Sultan R.A., Rahman M.A., Rushd S., Zendejboudi S., Kelessidis V. C., 2019, Validation of CFD model of multiphase flow through pipeline and annular geometries, *Particulate Science and Technology*, 37, 685-697.
- Visuri O., Wierink G.A., Alopaeus V., 2012, Investigation of drag models in CFD modeling and comparison to experiments of liquid–solid fluidized systems, *International Journal of Mineral Processing*, 104, 58-70.
- Vittorio Messa G., Malavasi S., 2014, Numerical prediction of particle distribution of solid-liquid slurries in straight pipes and bends, *Engineering Applications of Computational Fluid Mechanics*, 8, 356-372.
- Wang J., Wang S., Zhang T., Liang Y., 2013, Numerical investigation of ice slurry isothermal flow in various pipes, *International Journal of Refrigeration*, 36, 70-80.
- Xia B., Sun D.W., 2002, Applications of computational fluid dynamics (CFD) in the food industry: review, *Computers and Electronics in Agriculture*, 34, 5-24.